# Barriers to Translocation of Organic Ions in Phospholipid Membranes

**B. S. Prabhananda* and Mamata H. Kombrabail**

*Department of Chemical Sciences, Tata Institute of Fundamental Research, Mumbai 400 005, India*

*Received: April 27, 1998; In Final Form: June 22, 1998*

The hypothesis that a dominant barrier to the translocation of organic ions (such as carbonyl cyanide *m*-chlorophenylhydrazone (CCCP)) across phospholipid bilayer membranes is located between the "polar region" and "nonpolar region" of the membrane layer has been confirmed by the following observation: The rate of decay of the pH difference across soybean phospholipid vesicular membrane (ΔpH) increased substantially when the above substep was specifically catalyzed. In our strategy, the formation of the electroneutral ternary complex valinomycin−$M^+$−$CCCP^-$ ($M^+ = K^+$, $Cs^+$) affects this substep. Also, $CCCP^-$ ion translocation is facilitated by having an alternate path for the compensating charge flux of alkali metal ions through gramicidin channels. The observed enhancement behaviors on changing the lipid composition from soybean phospholipid (SBPL) to a mixture of PC + 6% PA, weak acid from CCCP to carbonyl cyanide 4-trifluoromethoxyphenylhydrazone (FCCP), and the metal ion from $K^+$ to $Cs^+$ are consistent with the predictions of the suggested mechanisms. The increase in the ΔpH decay rate on increasing the ionic strength confirms the Coulombic nature of a dominant interaction between the $CCCP^-$ ion and the lipid contributing to the kinetic barrier. Even though the gross features of the ion translocation barrier profile inferred by us are similar to that given in the literature, our results suggest the need to consider ion translocation across the phospholipid membrane to involve at least three substeps. This requires a refinement of the barrier profile given in the literature. In our experiments, the ΔpH was created by temperature jump, and observations on the ΔpH decay were made by monitoring the fluorescence from the pyranine entrapped inside the vesicles.

## Introduction

According to Mitchell's hypothesis,[1] hydrogen ion concentration difference across the membrane drives oxidative phosphorylation. Weak acids such as carbonyl cyanide *m*-chlorophenyl hydrazone (CCCP) and 2,4-dinitrophenol (DNP) uncouple oxidative phosphorylation by transporting $H^+$ across the membrane in the protonated state (CCCPH and DNPH), thereby facilitating the ΔpH decay. The $H^+$ transport cycle is completed by the back-translocation of anions ($CCCP^-$ and $DNP^-$) across the membrane. In the past, the kinetics of translocation of such organic ions and small polar molecules have been investigated in planar bilayer lipid membranes (BLM) from a study of electrical transients[2−10] and in vesicular membranes from spectroscopic observations.[11,12] The time domain data obtained in these studies have been analyzed assuming the translocation across the membrane to be a single-step process. The magnitude of the translocation rate constant depends on the "barrier" to translocation. The barrier profile is determined by the sums of various energy contributions associated with the interaction of the ion with the environment at different points on the membrane. In the literature, the electrostatic contributions to the barrier have been discussed in terms of Born energy[3,12−14] required to move the ion from an environment of dielectric constant $\epsilon_1$ to an environment of dielectric constant $\epsilon_2$ and image forces[12,14−16] experienced by the ion at the boundary of two different dielectric media. The hydrophobic interaction of the lipophilic ion with the membrane and the energy terms associated with the distortion of the closely packed membrane structure to accommodate the ion[10,12,14] also contribute to the barrier. In the past, profiles such as trapezoidal and rectangular barriers or barriers with a maximum in the core region of the bilayer have been preferred for specific BLM systems by comparing the predicted shapes of the current−voltage curves with data.[8,10,14,17] Also in liposomes, trapezoidal barrier has been used to explain the nonohmic conductance seen in the membrane potential driven $H^+/OH^-$ flux data.[18]

The barriers assumed in such studies do not take into account the possibility that the translocation across the membrane could be a multistep process with several maxima in the energy profile across the bilayer membrane (apart from the barriers at the aqueous medium−membrane interface). However, experimental data suggest a barrier profile similar to Figure 1: Reflectance data shows that a "trilple-layer model" with a "nonpolar" organic phase region between two "polar" regions is a more realistic description of the BLM.[19,20] In this model, the dielectric constants (and hence the refractive indices) of the "polar" and "nonpolar" regions are different. Therefore, from electrostatic considerations similar to that mentioned above, we expect an energy barrier between the "polar" to the "nonpolar" regions of BLM (Figure 1). Also, using temperature jump (T-jump) relaxation studies, Ruf[21] has inferred that the neutral *o*-methyl red molecules are exchanged between the membrane surface and nonpolar interior in a slower step, after binding to the vesicular membrane in a faster step. The rate constants evaluated from experimental data[21] show that the concentration of the neutral *o*-methylred in the nonpolar interior is nearly 4 times smaller than near the membrane surface. This observation requires us to expect a deeper potential well near the membrane surface in the "polar" region (due to Coulombic interaction with the dipole moment of the molecule) compared to the potential well in the "nonpolar" region (Figure 1). We can expect a qualitatively similar barrier profile for the organic ion translocation and hypothesize that ion translocation within the bilayer

10.1021/jp982020h CCC: $15.00 
Published on Web 10/01/1998

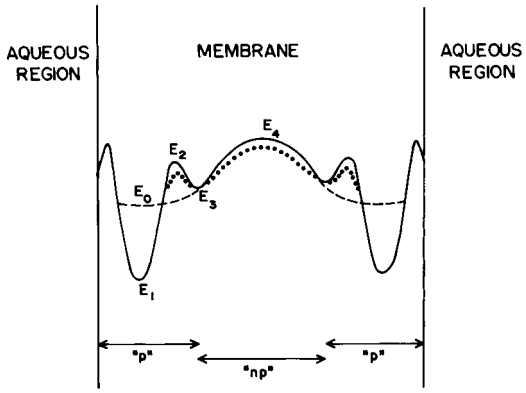


**Figure 1.** Suggested schematic representation of the energy barrier profile associated with the interaction of an organic ion with the environment in a phospholipid bilayer membrane. The broken line represents the change in the energy profile when the electrostatic contributions alone are reduced. (The Born energy term in the nonpolar region is assumed to be small and negligible.) Changes in the hydrophobic interactions also add to the energy changes. The dotted line is representative of the situation when all the three barriers are affected.

membrane involves at least three substeps: (1) translocation of the ion from the "polar region" to the "nonpolar region" in the first layer, (2) translocation from the "nonpolar region" of the first layer to the "nonpolar region" of the second layer, and (3) translocation from the "nonpolar region" to the "polar region" of the second layer. We can also consider the translocation as a multistep process, the "packed membrane structure" resisting the small step diffusional motion to different extents in different regions of the membrane and the electrostatic interactions also contributing to the "resistance" in the "polar region". Presumably, the experimental data reported in the literature are not adequate to infer such features of the barrier or "resistance to motion".

In the present work, the above hypothesis has been tested using the membrane permeant $CCCP^-$ as the organic anion and soybean phospholipid (SBPL) vesicles in aqueous solutions as model membrane systems in view of the data already available in the literature and other advantages of SBPL vesicular membranes mentioned elsewhere.[11,22−24] Representative experiments have also been carried out using vesicles prepared from phosphotidylcholine (PC) + 6% phosphatidic acid (PA) lipid mixtures.

**Strategy for Testing the Hypothesis.** Our strategy is based on choosing a membrane permeant species capable of dominantly affecting only one of the substeps of ion translocation and observing the consequent change in the effective translocation rate constant. The requirements of such a strategy are (a) a reliable method of estimating the effective translocation rate constant, (b) a method of isolating contributions to data from translocations involving the uncomplexed $CCCP^-$ ion, and (c) knowledge about all the factors that can affect data. The details of our strategy are described below.

In the CCCP mediated decay of the pH difference across the vesicular membrane (ΔpH), a fast transfer of $H^+$ from the aqueous medium on "one side" of the membrane to the $CCCP^-$ in the membrane is followed by rapid translocation of the electrically neutral CCCPH across the membrane. On the "second side" of the membrane, $H^+$ is released from CCCPH to the aqueous medium in a fast step and $CCCP^-$ is translocated back to the "first side" of the membrane (to restore the concentration of CCCP on the "first side"), completing the $H^+$ transport cycle. However, this process generates a membrane potential that opposes further $H^+$ transport cycles. For the ΔpH decay in liposomes this membrane potential has to be abolished by a compensating charge flux such as that of alkali metal ion, $M^+$.[25] Translocation of $M^+$ through the gramicidin channels in the membrane can provide the compensating charge flux.[11] At the gramicidin and $M^+$ concentrations used in our experiments, the $M^+$ transport through the channels is not the rate-limiting step of ΔpH decay.[11,26] In such a system, at sufficiently high concentrations of CCCPH, the rate-limiting step of ΔpH decay is the translocation of $CCCP^-$ across the membrane, and the ΔpH relaxation rate ($=1/\tau$) will be proportional to the concentration of the uncomplexed $CCCP^-$ in the membrane and its "effective translocation rate constant", $k_c$.[11] In a three-step translocation, such as that expected for the barrier profile of Figure 1, the magnitude of $k_c$ will be determined by the rate constants (proportional $\exp\{(E_1 - E_2)/RT\}$, $\exp\{(E_3 - E_4)/RT\}$, and $\exp\{(E_3 - E_2)/RT\}$) associated with the three substeps. If the effective charge on $CCCP^-$ seen by the membrane environment is somehow reduced, the depth of the potential wells near the membrane surface and the barrier maximum between the "polar" and "nonpolar" regions will be reduced, changing the energy profile similar to that shown by the broken line in Figure 1. In this case, the rate constant associated with the translocation of $CCCP^-$ in the "first substep" will increase. Furthermore, if this substep is a significant rate-determining step, the effective translocation rate constant $k_c$ will increase.

A reduction in the effective charge seen by the membrane environment can be achieved by complexing $CCCP^-$ with a positively charged species. In the present work, we have used the alkali metal ion complexes of valinomycin (Val−$M^+$, $M^+ = K^+, Cs^+$) as the membrane permeant positively charged species capable of forming electroneutral complexes Val−$M^+$−$CCCP^-$. If the reduction in the electrostatic terms dominates the changes in the energy profile associated with the complex formation, there will be an increase in the rate constant of the first substep, and we can have a situation as shown schematically by the following reactions.

$$(CCCP^-)_p \rightarrow (CCCP^-)_{np} \quad \text{(slow)}$$

$$(CCCP^-)_p + (\text{Val-}M^+)_p \rightleftharpoons (\text{Val}-M^+-CCCP^-)_p \rightarrow (\text{Val}-M^+-CCCP^-)_{np} \quad \text{(fast)}$$

where the subscripts "p" and "np" refer to "in the polar region" and "in the nonpolar region", respectively. After the fast substep, $CCCP^-$ can translocate from the nonpolar region of the first layer to the second layer in the rate-limiting "second substep" in the complexed state itself (i.e., as Val−$M^+$−$CCCP^-$). Such a mechanism does not require a charge-compensating flux of $M^+$ through gramicidin channels since $M^+$ is carried by the ternary complex itself. Alternatively, the second substep may involve dissociation of the ternary complex in the nonpolar region of the first layer either by a fast unimolecular process (scheme I) or a fast dissociation aided by a second coordinating $CCCP^-$ from the polar region (scheme II) as shown below and the subsequent translocation as the uncomplexed $CCCP^-$.

$$(\text{Val}-M^+-CCCP^-)_{np} \rightarrow (\text{Val}-M^+)_{np} + (CCCP^-)_{np} \quad \text{(I)}$$

$$(CCCP^-)_p + (\text{Val}-M^+-CCCP^-)_{np} \rightarrow (CCCP^--\text{Val}-M^+)_p + (CCCP^-)_{np} \quad \text{(II)}$$

Since the electrostatic interaction between the organic ion and the nonpolar region is negligible, the main energy contribution to the barrier in the nonpolar core region comes from the distortion of the "close packing" of the lipid molecules in the membrane to accommodate the ion. Thus, in the second substep, the $CCCP^-$ ion is translocated within the nonpolar region more efficiently in the dissociated state (as the ion $CCCP^-$) than as the electroneutral ternary complex, since the ion is smaller in size. In both schemes given above, the contribution to $1/\tau$ is proportional to the concentration $[Val-M^+-CCCP^-]_m$. In "scheme II" the contribution to $1/\tau$ is also proportional $[CCCP^-]_m$ (the subscript "m" referring to "in the membrane"):

$$1/\tau_1 = A_1[Val-M^+-CCCP^-]_m \quad (1)$$

$$1/\tau_2 = A_2[Val-M^+-CCCP^-]_m[CCCP]_m \quad (2)$$

The detailed expressions for $1/\tau_1$ and $1/\tau_2$ are given in the Appendix (eqs A9 and A11). After taking note of other factors that contribute to the observed $1/\tau$ (given below), the characteristic features of $1/\tau_1$ and $1/\tau_2$ can be used as signatures to identify the existence of such schemes.

In our experiments, the following three known mechanisms (in which fast $M^+$ transport through the gramicidin channels provides the compensating charge flux) make small contributions to $1/\tau$: (i) from $H^+$ transport through gramicidin channels and $OH^-$ propogation along water chains in the membrane, $1/\tau_G$ (eq A5);[26] (ii) from a mechanism in which $CCCP^-$ translocates unaided by valinomycin (VAL) (eq A6);[11] (iii) from a mechanism involving the translocation of $CCCP^-$ as its complex with VAL, $Val-CCCP^-$ (eq A7).[11] With the help of the parameters determined in our earlier works[11,26] or from typical $1/\tau$ data obtained earlier, we can show that such contributions are negligibly small compared to the observed $1/\tau$ in the experiments described below. Also, using nigericin mediated ΔpH decay as probe, we had noted that at the concentrations of gramicidin used in our experiments changes in translocation rate constants due to gramicidin induced changes in the membrane order are negligible.[11]

However, as mentioned above, both $M^+$ and $CCCP^-$ can also be translocated across the membrane as the electroneutral complex $Val-M^+-CCCP^-$ without requiring gramicidin channels for the compensating charge flux of $M^+$. In our experiments nonnegligible contributions to $1/\tau$ comes from this mechanism.[27] This contribution ($=1/\tau_{VC}$, (eq A2)) can be determined either by calculation or from the $1/\tau$ data obtained in the absence of gramicidin. Thus, the dominant increase in $1/\tau$ on adding gramicidin ($=1/\tau_{ch}$) can be assigned to mechanisms of ΔpH decay, in which uncomplexed $CCCP^-$ is translocated in a substep.

In the mechanism of our strategy, $CCCP^-$ is translocated as the electroneutral complex $Val-M^+-CCCP^-$ in the first substep (with higher rate constant compared to that of uncomplexed $CCCP^-$), and the second substep involves translocation of the uncomplexed $CCCP^-$ ion after the dissociation of the ternary complex by scheme I or II. The observation of a significant $1/\tau_{ch}$ confirms the success of our strategy for enhancing the rate of one of the $CCCP^-$ translocation substeps. In our anlaysis of the data, the changes in translocation rate constants due to membrane permeant species induced changes in the membrane order have also been included using the experimentlly determined factor $F$ given in the Appendix (eq A4).

## Materials and Methods

SBPL vesicle solutions with 2 mM pyranine inside and other concentration conditions as given in the figure legends were prepared from acetone-washed asolectin (Sigma) following the procedure described elsewhere.[22,23] Lipid mixtures of L-α-phosphotidylcholine (PC) from frozen egg yolk + 6% L-α-phosphatidic acid (PA) sodium salt from egg yolk lecithin (Sigma) were also used to prepare vesicles. The pH of *N*-(acetamido)-2-aminoethanesulfonic acid (ACES) buffer and phosphate buffer was adjusted using concentrated KOH/HCl. In our experiments KCl and CsCl were used to regulate alkali metal ion concentrations in vesicle solutions. Stock solutions of 1, 10, or 40 mM CCCP and carbonyl cyanide 4-trifluoromethoxyphenylhydrazone (FCCP), 1 or 10 mM VAL, and 5 or 15 mM gramicidin (Sigma) were prepared in ethanol. They were added in microliter amounts to vesicle solutions with vortex stirring. The apparent p*K* of FCCP in SBPL membrane (~6.45) was determined from the pH dependence of the optical density at 380 nm. Mixtures of tris(hydroxymethyl)aminomethane (TRIS), 2-(*N*-morpholine)ethanesulfonic acid (MES), and acetate buffers were used in such a study. T-jump was used to create ΔpH (~0.02), and the ΔpH decay was observed at 23 ± 1.5 °C by monitoring the fluorescence from the pH indicator pyranine entrapped inside vesicles.[22,23] The ΔpH relaxation times $\tau$ were measured (within the error limit of ±20%) by comparing the observed trace with those obtained from a calibrated exponential generator.[23] At least four relaxation traces were examined from a given sample to ensure the reproducibility of the relaxation times within the 10% error limit. To minimize scatter of data due to small differences in vesicle preparations, all data points under a given experimental condition were obtained using the same vesicle preparation. The observed concentration dependences were confirmed from at least two independent sets of vesicle preparations. The sizes of vesicles were regulated to those in previous works by monitoring the optical density at 700 nm and reproducing standard relaxation traces within the limits of error.[23] The relaxation times obtained in our experiments (using different vesicle preparations and different concentration conditions) could be predicted from theoretical equations using the parameters given below (with variations within 30%).

## Results

**Enhancement of CCCP Mediated ΔpH Relaxation Rate on Adding Gramicidin ($=1/\tau_{ch}$) with VAL in the Membrane.** In the discussions below, the concentrations given with subscripts "0" refer to concentrations estimated with respect to the volume of the vesicle solution (see eq A1). In the absence of gramicidin, typical variation of $1/\tau$ on varying $[CCCP]_0$ keeping $[VAL]_0$ small and constant in SBPL vesicle solutions containing 100 mM KCl has been given in the literature[27] for the pH range 6−7.5. Such data can also be reproduced by the expression for $1/\tau_{VC}$ (eq A2) using the parameters determined earlier.[27] In Figure 2, $1/\tau$ data in the absence of gramicidin have been plotted using eq A2 for three pH conditions. Figure 2 also gives the corresponding $1/\tau$ data experimentally observed on adding gramicidin.

The magnitudes of increase in $1/\tau$ on adding gramicidin given in Figure 3($=1/\tau_{ch}$, calculated using the data in Figure 2) show features expected from a transport scheme in which the uncomplexed $CCCP^-$ translocation is a substep in the rate-limiting step of the ΔpH decay: (i) compensating charge flux of $M^+$ through the gramicidin channels is necessary to enable this contribution; (ii) $1/\tau_{ch}$ shows nearly a linear increase with

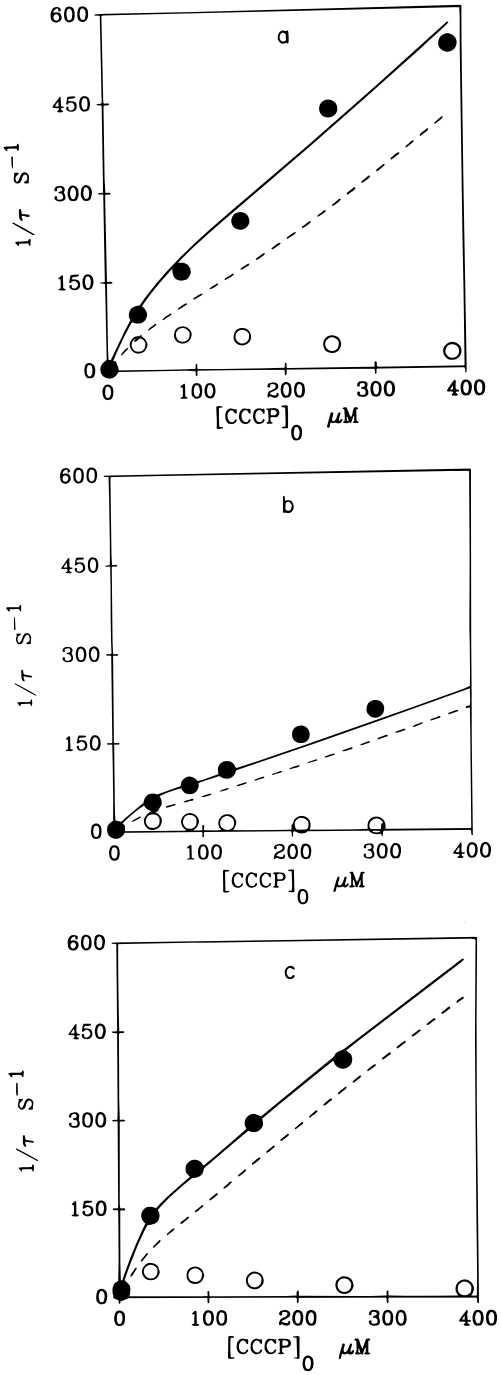


**Figure 2.** Dependence of ΔpH relaxation rate $1/\tau$ on $[CCCP]_0$ with $[VAL]_0$ small and constant in SBPL vesicle solutions containing 100 mM KCl. The $1/\tau$ data with $[Gram]_0 = 0$ (○) was calculated using the expression for $1/\tau_{VC}$ (eq A2) as described in the text. $1/\tau$ data with $[Gram]_0 = 20\ \mu M$ (●) was obtained from experiments. Inside vesicles 50 mM phosphate buffer and outside vesicles was 50 mM ACES buffer. (a) pH ∼ 6.18, $[VAL]_0 = 2\ \mu M$, [lip] = 5.3 mM; (b) pH ∼ 7, $[VAL]_0 = 1\ \mu M$, [lip] = 4.5 mM; and (c) pH ∼ 7.5, $[VAL]_0 = 3\ \mu M$, [lip] = 5.3 mM. Contributions from $1/\tau_{VC}$ (eq A2), from scheme I, $1/\tau_1$ (eq A9), and from scheme II, $1/\tau_2$ (eq A11) were included in the calculation of solid lines. Broken lines were calculated excluding the contribution from scheme I. Parameters given in the text were used in these calculations.

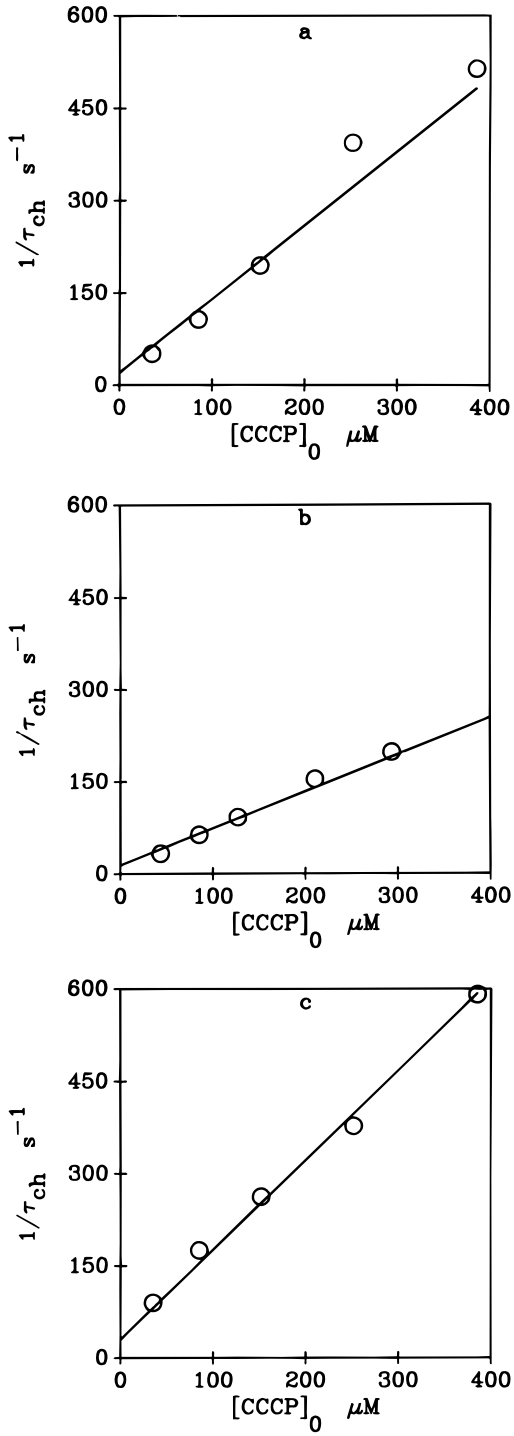


**Figure 3.** Change in the ΔpH relaxation rate on adding gramicidin ($=1/\tau_{ch}$) calculated from the data given in Figure 2 and plotted against $[CCCP]_0$ for (a) pH ∼ 6.18, (b) pH ∼ 7, and (c) pH ∼ 7.5. The solid lines were calculated using $1/\tau_{ch} = 1/\tau_1 + 1/\tau_2$ (eqs A9 and A11) and the parameters given in the text.

$[CCCP]_0$; (iii) the plots obtained with $[VAL]_0$ = constant show that their slopes are not sensitive to the choice of pH in our pH range (∼6−8). The latter two behaviors can be understood using the experimental conditions given in the figure captions and by noting that $(F \ln 10/b_i)\{K_{H4}/(K_{H4} + [H^+])\}$ in eq A11 does not show large variation with $[CCCP]_0$ and pH (30−40 $M^{-1}$ at pH ∼ 6.18, ∼ 30 $M^{-1}$ at pH ∼ 7, and 40−35 $M^{-1}$ at pH ∼ 7.5).

The above three features are similar to that observed earlier and were attributed to the ΔpH decay rate-limiting step of $CCCP^-$ translocation in the absence of VAL in the membrane.[11] However, for a given $[CCCP]_0$, $1/\tau_{ch}$ observed with VAL in the membrane (in this work) is much larger than the $1/\tau$ observed in the absence of VAL,[11] implying an enhancement in the effective translocation rate constant of $k_c$ of $CCCP^-$ by the

presence of VAL. Also, from a knowledge of the dissociation constant of Val−$K^+$−$CCCP^-$ determined in an earlier work,[27] we can say that, at the high $[CCCP]_0$ used in our experiments, almost all the VAL added is present in the membrane as the ternary complex. Thus, the mechanism of enhancement of $k_c$ must involve the ternary complex and should predict a near linear dependence of $1/\tau_{ch}$ on $[CCCP]_0$ at the high $[CCCP]_0$ of Figures 2 and 3. Scheme II and eq A11 derived on the basis of this scheme satisfy these requirements.

The intercepts of the near-linear plots of Figure 3 on the $1/\tau_{ch}$ axis are beyond the limits of errors. They can be attributed to contributions from scheme I (eq A9). The solid lines of Figure 2 (which agree with the observed data) have been obtained using the parameters given in the literature[11,26,27] with $k_2 \sim 3.2 \times 10^3\ s^{-1}$, $k_{21} \sim 3 \times 10^3\ s^{-1}$, and $k_{22} \sim 1.5 \times 10^5\ M^{-1}\ s^{-1}$ in eqs A2, A9, and A11. (See eqs A8 and A10 for the definition of rate constants.)

**Additional Concentration Dependences Predicted by the Proposed Mechanisms.** (a) In the above analysis of data (obtained in SBPL vesicles containing CCCP, VAL, and gramicidin), we have identified the three dominant contributions to $1/\tau$ to be the contributions given by eqs A2, A9, and A11. All these three contributions are proportional to the concentration of the Val−$M^+$−$CCCP^-$ complex (which depends on $[VAL]_0$). Therefore, $1/\tau$ should be proportional to $[VAL]_0$. Figure 4a confirms such a prediction.

(b) Figure 4b shows that the pH dependence of $1/\tau$ obtained in the experiments with high $[CCCP]_0$ is consistent with the behavior predicted by adding the above-mentioned three dominant contributions (eqs A2, A9, and A11).

(c) In the experiments with small $[CCCP]_0$ and sufficiently high $[VAL]_0$ almost all the added CCCP can be expected to be complexed with VAL. Therefore, we cannot expect any contribution from scheme II. Also under these conditions, because of the absence of complexation with a second $CCCP^-$ from the polar region, the recombination with the Val−$M^+$ released in the nonpolar region reduces the probability of uncomplexed $CCCP^-$ translocation even after dissociation by scheme I. Thus, with small $[CCCP]_0$ and high $[VAL]_0$ we should not see significant enhancement of $1/\tau$ on adding gramicidin. The $1/\tau$ obtained on varying $[VAL]_0$ keeping $[CCCP]_0$ small (Figure 4c) is consistent with this prediction.

**Predictions Based on the Nature of the Barrier in Our Hypothesis.** (a) In our hypothesis, in the absence of complexation with Val−$M^+$, the dominant contribution to the translocation barrier comes from the Coulombic interaction between $CCCP^-$ and the polar region of the membrane. If this is true, by increasing the ionic strength in the membrane (by the increase of [KCl] in vesicle solutions), we should be able to reduce the Coulombic interaction and increase the translocation rate of $CCCP^-$. In the CCCP mediated $\Delta$pH decay (in the absence of VAL) observed on adding gramicidin, $1/\tau$ is proportional to the translocation rate of $CCCP^-$.[11] Analysis of $1/\tau$ of Figure 5a using eqs A1 and A3−A6 shows that the $CCCP^-$ translocation rate constant increases from ~1.5 to 3.4 $s^{-1}$ on increasing [KCl] from 100 to 300 mM, consistent with the aforementioned prediction.

(b) Addition of anesthetics such as chloroform to vesicle solutions perturbs the membrane structure and increases transport rates presumably by loosening the "close-packed structure" which lowers the barriers or decreases the resistance to translocation.[26,28] As explained above, in the CCCP-mediated $\Delta$pH decay with VAL in the membrane, the rate-limiting substep of $CCCP^-$ translocation across the nonpolar region ("second substep") can take place as (i) the Val−$M^+$−$CCCP^-$ complex in the absence of compensating charge flux through gramicidin channels and (ii) also as the uncomplexed $CCCP^-$ when gramicidin channels are present. Thus, in these situations (Figure 6a,b or Figure 5c,d) only the lowering of the barrier in the nonpolar region by $CHCl_3$ causes an increase in $1/\tau$. On

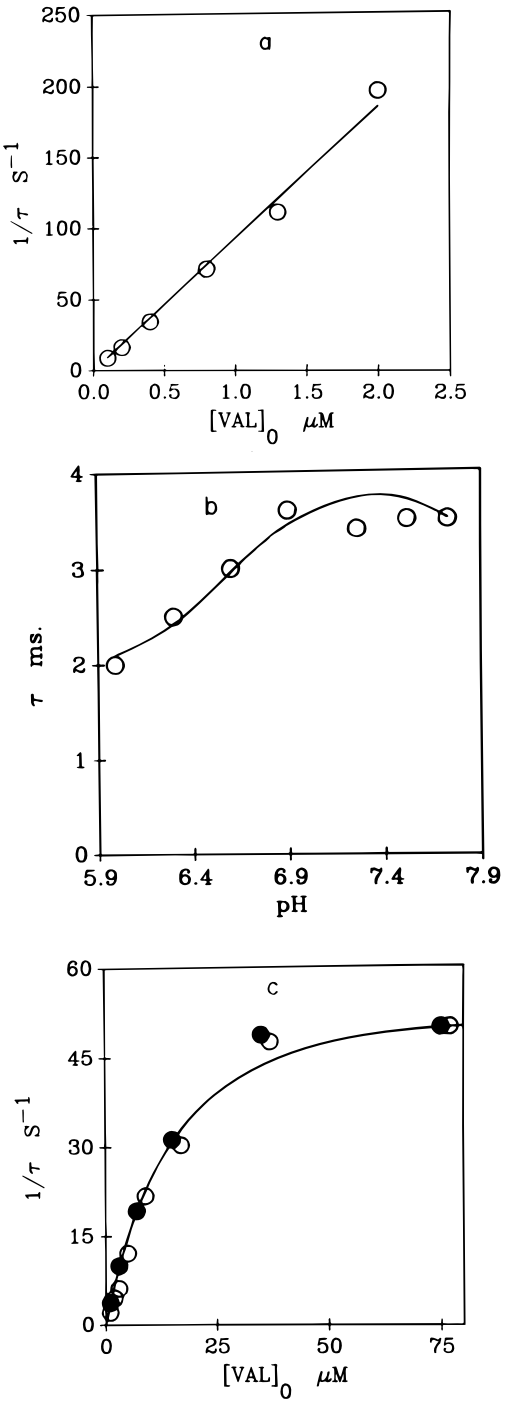


**Figure 4.** Additional $\tau$ data at pH ~ 7, confirming the predictions (see text) in SBPL vesicle solutions containing 100 mM KCl and 25 mM ACES as outside buffer. (a) Dependence of $1/\tau$ on $[VAL]_0$ with high $[CCCP]_0$ (=83 $\mu$M), [lip] = 4.2 mM, inside buffer 50 mM phosphate, $[Gram]_0 = 20\ \mu$M. (b) pH dependence of $\tau$ observed with small $[VAl]_0$ (=2.2 $\mu$M) and high $[CCCP]_0$ (=83 $\mu$M), [lip] = 5.6 mM, inside buffer 2 mM phosphate, $[Gram]_0 = 45\ \mu$M. (c) Dependence of $1/\tau$ on $[VAL]_0$ with $[CCCP]_0 = 2\ \mu$M, [lip] = 5 mM, inside buffer 50 mM phosphate. The data with $[Gram]_0 = 0$ (○) and with $[Gram]_0 = 20\ \mu$M (●). Solid lines were calculated by following the procedure described in the caption of Figure 2.

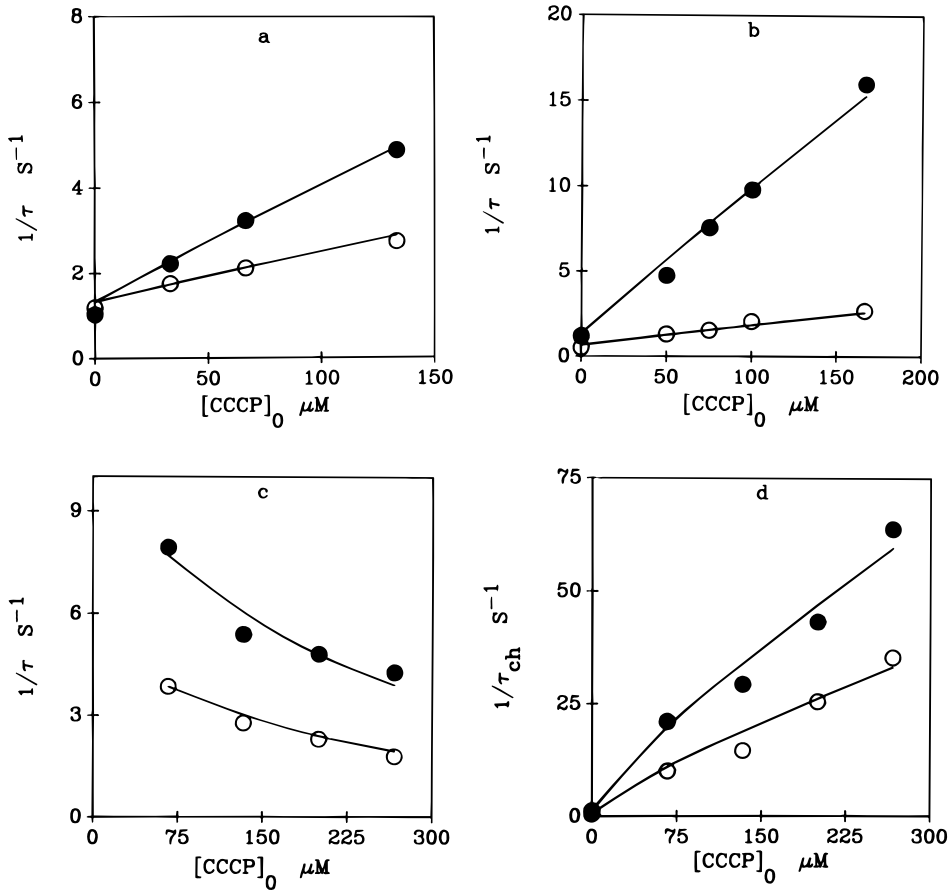


**Figure 5.** Dependence of ΔpH relaxation rates on $[CCCP]_0$ in SBPL vesicle solutions. (a) At [KCl] = 100 mM (○) and 300 mM (●) with [lip] = 3.5 mM and $[Gram]_0 = 25\ \mu M$. (b, c, d) In 5.2 mM SBPL vesicle solutions with [KCl] = 100 mM, $1/\tau$ before adding $CHCl_3$ (○) and after adding $CHCl_3$ 4 μL/mL (●); (b) $[VAL]_0 = 0$, $[Gram]_0 = 17\ \mu M$; (c) $[VAL]_0 = 0.2\ \mu M$, $[Gram]_0 = 0$; (d) $[VAL]_0 = 0.2\ \mu M$, $[Gram]_0 = 17\ \mu M$. In these experiments, 50 mM phosphate buffer was inside vesicles, and 25 mM ACES was outside vesicles at pH ~ 7.5.

the other hand, in the absence of VAL (Figures 5b and 6c) when the first substep also contributes to the limiting of the rate, the lowering of the barrier between the polar and nonpolar regions by the added $CHCl_3$ is expected to cause an increase in $1/\tau$ by an additional factor. (The effective $k_c$ involves the product of rate constants of the two substeps[29] in the numerator and their sum in the denominator.) Experimental observations are consistent with such an expectation: the slope of the $1/\tau_{ch}$ against $[CCCP]_0$ plot increases by a smaller factor on adding chloroform in Figure 5d than the increase seen in the slopes of Figure 5b plots.

**Predictions about the Relative Contributions from the Two Schemes.** Our strategy is based on a general description of the barrier in a phospholipid bilayer membrane. Therefore, the enhancement of $1/\tau$ observed on adding gramicidin to SBPL vesicles containing VAL, $K^+$, and CCCP should be observable in the experiments (a) with vesicles prepared from other phospholipids, (b) with other weak acids similar to CCCP, and (c) with other alkali metal ions that form complexes with VAL, albeit the relative contributions from the two schemes could be different. The following observations confirm such a prediction.

(a) In an environment where the probability of formation of the $Val-K^+-CCCP^-$ is small even at the high $[CCCP]_0$ used in our experiments, the probability of formation of the intermediate state of scheme II, $(CCCP^-)_p$:$(Val-M^+-CCCP^-)_{np}$, will be even smaller. In such a situation the contribution to $1/\tau_{ch}$ can be predicted to be mainly from scheme I. Such an environment can be expected in vesicles prepared from PC + 6% PA, since the apparent dissociation constant of $Val-K^+-CCCP^-$ is ~30 times and the apparent metal dissociation constant of $Val-K^+$ is ~3 times the values observed in SBPL vesicles. The above prediction was verified from experiments on 5.3 mM PC + 6% PA vesicle solutions with 2 mM phosphate inside and 25 mM ACES outside vesicles at pH ~ 7.5 (experimental conditions chosen to facilitate comparison with the data given in Figure 5f of ref 27). Thus, $\tau$ decreased from 24 to 18 ms on adding 17 μM gramicidin to vesicle solutions containing $[VAL]_0 = 8\ \mu M$ and $[CCCP]_0 = 32\ \mu M$ as well as $[VAL]_0 = 16\ \mu M$ and $[CCCP]_0 = 16\ \mu M$. (In PC + 6% PA vesicles the concentration of the ternary complex at these conditions is nearly proportional to the product $[VAL]_0[CCCP]_0$ even at the high concentrations used. The observed $1/\tau_{ch}$ (=14 $s^{-1}$) is given by eq 1 in these cases.)

(b) The mechanisms given by schemes I and II should also manifest themselves when a different uncoupler (but similar to CCCP) such as FCCP is used. Figure 7a shows the variation of $1/\tau$ with $[FCCP]_0$ oberved in the absence of gramicidin and on adding gramicidin, keeping $[VAL]_0$ small, in SBPL vesicle solutions at pH ~ 7. The observed behaviors are similar to those seen with CCCP and confirm the existence of schemes I and II in this system also. An analysis of the data yielded the $FCCP^-$ dissociation constant of $Val-K^+-FCCP^-$, $K_1 = 2.5$ mM (which is slightly higher than ~2 mM observed with CCCP), $k_2 = 5 \times 10^3\ s^{-1}$ for the translocation rate constant of the ternary complex $Val-K^+-FCCP^-$ (which is higher than $\sim 3.2 \times 10^3\ s^{-1}$ obtained with CCCP), $k_{21} = 3 \times 10^3\ s^{-1}$, and $k_{22} = 1.75 \times 10^5\ M^{-1}\ s^{-1}$.

(c) Since changing $M^+$ changes the interactions of $M^+$ with VAL and $CCCP^-$ in the ternary complex, we should expect the relative contributions from the two mechanisms to be

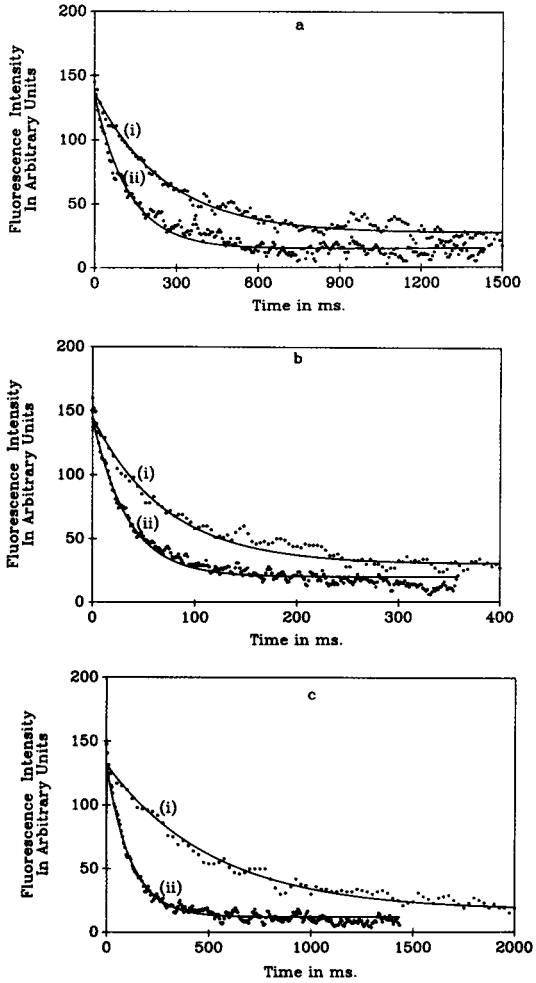


**Figure 6.** ΔpH relaxations observed (i) before adding $CHCl_3$ and (ii) after adding 4 $\mu$L of $CHCl_3$ to 1 mL of 5.2 mM SBPL vesicle solutions. [KCl] = 100 mM, inside vesicles 50 mM phosphate buffer and outside 25 mM ACES buffer at pH ~ 7.5. (a) $[VAL]_0 = 0.2$ $\mu$M, $[CCCP]_0 =$ 67 $\mu$M, $[Gram]_0 = 0$; (b) $[VAL]_0 = 0.2$ $\mu$M, $[CCCP]_0 = 67$ $\mu$M, $[Gram]_0 = 17$ $\mu$M; (c) $[VAL]_0 = 0$, $[CCCP]_0 = 75$ $\mu$M, $[Gram]_0 = 17$ $\mu$M. The superposed single exponentials were calculated using relaxation times $\tau = 260$ and 126 ms for (i) and (ii) of (a), $\tau = 72$ and 35 ms for (i) and (ii) of (b), and $\tau = 525$ and 120 ms for (i) and (ii) of (c).

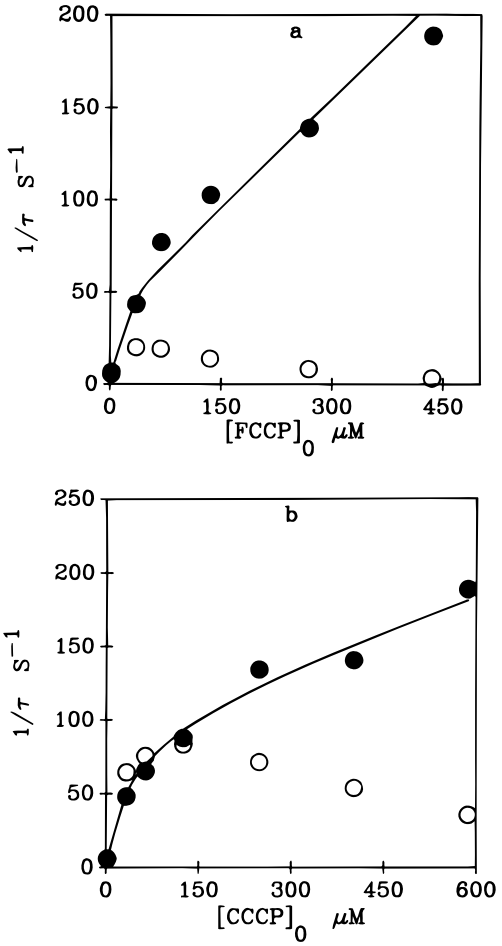


**Figure 7.** (a) Dependence of $1/\tau$ on $[FCCP]_0$ in SBPL vesicle solutions containing 100 mM KCl, at pH ~ 7, $[VAL]_0 = 0.75$ $\mu$M, [lip] = 4.6 mM, inside buffer 50 mM phosphate and outside buffer 25 mM ACES. (b) Dependence of $1/\tau$ on $[CCCP]_0$ in SBPL vesicle solutions containing 100 mM CsCl, at pH ~ 7.45, $[VAL]_0 = 2.9$ $\mu$M, [lip] = 4.6 mM. Inside buffer was a mixture of 0.25 mM ACES and 0.25 mM TRIS, and buffer outside vesicles was 25 mM TRIS. In both (a) and (b), $1/\tau$ data with $[Gram]_0 = 0$ (○) and with $[Gram]_0 = 20$ $\mu$M (●) are experimental. Solid lines were calculated using the parameters and equations given in the text.

dependent on the choice of $M^+$. Since the $K^+/Na^+$ selectivity of VAL is high, impractical concentrations of $CCCP^-$ are required to test the "hypothesis" if $M^+ = Na^+$. In our experiments, we have used $Cs^+$ which is larger than $K^+$ in size. The metal ion dissociation constant of Val−$M^+$ is nearly 3 times higher when $M^+ = Cs^+$ than when $M^+ = K^+$.[30] The data obtained using $M^+ = Cs^+$, given in Figure 7b at pH ~ 7.5, also show substantial increases in $1/\tau$ on adding gramicidin. From an analysis of $1/\tau$ data given in Figure 7b, assuming the translocation rate constant of the ternary complex to be unchanged on changing $M^+$ ($k_2 = 3.2 \times 10^3$ $s^{-1}$), we get $K_1 =$ 4 mM (which is twice that with $K^+$), $k_{21} \sim 0$, and $k_{22} \sim 2.2 \times 10^4$ $M^{-1}$ $s^{-1}$ (which are significantly smaller than that obtained with $K^+$).

## Discussion

**Elimination of Other Explanations of "Enhancement".** Since the "enhancement of $1/\tau$" discussed in this work is a consequence of the addition of gramicidin to the membrane, it may be suggested that the rate-limiting step of the additional contribution $1/\tau_{ch}$ is associated with proton/metal ion transport through the gramicidin channels. In such a hypothesis the experimental observations discussed above can perhaps be explained by invoking a suitable dependence of "the duration for which the channel is open" on $[VAL]_0$, $[CCCP]_0$, pH, and ionic strength. This hypothesis can be eliminated in view of the following observations: (i) In such a mechanism, the magnitude of the dominant contribution to $1/\tau_{ch}$ is expected to be proportional to gramicidin concentration even in the presence of carriers. Typical data obtained by varying gramicidin concentration (reported in Figure 1 of ref 31 and confirmed by us by independent experiments) are not consistent with such an expectation. (A small gramicidin concentration dependence of $1/\tau$ seen in such data can be attributed to an independent mechanism in which proton transport through the channels is the rate-limiting step (eq A5). An estimate of such a contribution can be obtained from the data in the absence of carriers.[26]) (ii) Earlier ΔpH decay studies[26] have shown that additions of chloroform to vesicle solutions (at concentrations used in our present experiments) do not affect transports through gramicidin channels significantly. Thus, our observations on the chloroform induced changes in $\tau$ also do not favor the above hypothesis.

If $1/\tau_{ch}$ can be attributed to gramicidin induced changes in membrane properties, there should be a significant dependence

of $1/\tau_{ch}$ on gramicidin concentration. The data given in Figure 1 of ref 31 are not consistent with such an expectation. Our results using nigericin-mediated ΔpH decay also confirm this conclusion.

The gramicidin concentrations used in our experiments are sufficiently small to ensure negligible contributions from the above mechanisms. However, they are adequate to ensure compensating charge flux needed by other mechanisms. This becomes possible since alkali metal ion transport through the channels is fast compared to the rate-limiting step of ΔpH decay at the metal ion concentrations used in our experiments. (In such a situation also $1/\tau$ does not depend on gramicidin concentration.)

Another alternative explanation of $1/\tau_{ch}$ which has appeared in the literature[31] is based on the mechanism in which (a) the ternary complex $Val-K^+-CCCP^-$ facilitates only the translocation of $CCCP^-$ and (b) in the absence of gramicidin channels $K^+$ translocation requires sufficient concentration of $Val-K^+$ (uncomplexed with $CCCP^-$). Thus, in this explanation, because of the formation of $Val-K^+-CCCP^-$, the concentration of $Val-K^+$ decreases on increasing $[CCCP]_0$ and $K^+$ translocation becomes the rate-limiting step of ΔpH decay at sufficiently high $[CCCP]_0$. On adding gramicidin $1/\tau$ increases because $K^+$ is rapidly translocated through the alternative path of gramicidin channels, and $K^+$ translocation ceases to be the rate-limiting step. With sufficient gramicidin in the membrane, the rate-limiting step in this mechanism will then be the $CCCP^-$ translocation as the electroneutral complex $Val-K^+-CCCP^-$. Two crucial predictions can be made on the basis of such a hypothesis: (i) At sufficiently high $[CCCP]_0$, in the absence of gramicidin, $[Val-K^+]$ and hence $1/\tau$ should increase on increasing $[K^+]$. The experimental observations are contrary to this prediction.[27] (ii) With $[VAL]_0$ small, $[Val-M^+-CCCP^-]$ will reach a saturating value at sufficiently high $[CCCP]_0$. Saturating concentrations of similar magnitudes can also be obtained for the rate-limiting species $Val-K^+-CCCP^-$ with an appropriate small value for $[CCCP]_0$ and sufficiently high $[VAL]_0$.[27] If the above hypothesis that the rate-limiting step on adding gramicidin is the translocation of $Val-K^+-CCCP^-$ is valid, the magnitudes of $1/\tau$ observed on adding gramicidin in both the situations mentioned above should be similar. Data obtained in the present work show much larger $1/\tau$ in the "first situation" contrary to the prediction.

**Observations That Favor Our Explanation of the "Enhancement".** In our explanation, the $1/\tau_{ch}$ contribution comes from an alternate path of $CCCP^-$ translocation: The first substep of transfer from the polar region to the nonpolar region is fast since this region is traversed as an electroneutral complex. The overall rate of translocation is limited by the second substep in which the ternary complex dissociates and the uncomplexed $CCCP^-$ ion traverses the nonpolar core region of the bilayer membrane. Our data have shown the characteristic features expected from such a mechanism: (i) The $\tau$ data obtained in the temperature range 10−25 °C shows a decrease in the activation energy associated with the translocation of the uncomplexed $CCCP^-$ ion from ∼13 to ∼4 kcal/mol. This is expected in view of the reduction in the electrostatic contributions to the barrier in the first substep. (ii) The dependence of the magnitude of $1/\tau_{ch}$ on the choice of $M^+$ ($K^+$ or $Cs^+$) supports our contention that $M^+$ bound species (ternary complexes in our case) are involved in the rate-limiting step. (iii) The need for the compensating charge flux through the gramicidin channels is indicative of the translocation of an uncomplexed ion in a substep of the rate-limiting step. (iv) The pH and $[CCCP]_0$ dependences of $1/\tau_{ch}$ are similar to that seen for $1/\tau$ when translocation of uncomplexed $CCCP^-$ had limited the ΔpH decay rate in the absence of VAL.[11]

**Conclusions about the Translocation of an Organic Ion in the Bilayer Membrane.** In the literature, translocation of ions within the membrane has been described either by the classical electrodiffusion approach using the Nernst−Planck equation[10,15] or using the formalism of chemical kinetics.[2,10] In the Nernst−Planck approach, the ion flux across the membrane is expressed in terms of the diffusion coefficient and potential energy of the ion. In this description our results imply two distinct regions of ion translocation across the membrane: (i) A region where electrostatic interactions dominantly determine the diffusion coefficient. The diffusion rate in this region can be increased by traversing this region in the form of an electroneutral complex. (ii) A second region where electrostatic interactions are less important and the diffusion of a smaller molecule with less distortion of the membrane structure is preferred. In the "chemical kinetics description" our results suggest the need to refine the barrier profiles given in the literature[10] by including the features suggested in Figure 1 and to describe the translocation of the ion from one layer to the second layer in terms of at least two kinetic steps, with one effective rate constant (for the overall translocation) needed to account for the data.

## Appendix

In the discussions below the subscripts "0", "i", "il", and "el" refer to concentrations with respect to the total volume of the vesicle solution, in the aqueous medium inside vesicles, and in the inner and outer layers of the vesicular membrane, respectively.

If the membrane permeant species "CR" is mainly partitioned to the membrane, its average concentration in the inner layer of the SBPL vesicles $[CR]_{il}$ can be expressed in terms of its concentration $[CR]_0$ estimated using the vesicle solution volume and [lip], the lipid concentration (see eq A2 of ref 27).

$$[CR]_{il} = 0.95[CR]_0/[lip]\ M \tag{A1}$$

"CR" may be partitioned into different extents in the "polar region" and "nonpolar region". Nevertheless, both $[CR]_p$ and $[CR]_{np}$ are proportional to $[CR]_{il}$. These proportionality constants are incorporated in the apparent rate constants such as $k_{21}$ and $k_{22}$ in the equations given below in terms of average concentrations $[CR]_{il}$ or $[CR]_0$.

In our strategy to test the hypothesis about the substeps in ion translocation across membrane, we have to first measure the ΔpH relaxation rate $1/\tau_{VC}$ due to VAL and CCCP in SBPL vesicle solutions containing KCl or CsCl. Theoretical analysis, experimental data determined earlier,[27] and the data given below show that the dominant contribution to $1/\tau_{VC}$ can be accounted for by the following expression.

$$1/\tau_{VC} \approx \frac{F\,(\ln 10/b_i)k_2[Val-M^+-CCCP^-]_{il}}{1 + \{[CCCP^-]_{il}([M^+]/K_M^*) + [Val-M^+]_{il}K_{H4}\}\{Fk_2/(k_1K_1)\}} \tag{A2}$$

In eq A2, $k_1$ (∼$2 \times 10^5$ $s^{-1}$) is the translocation rate constant of CCCPH and $k_2$ (∼$3.2 \times 10^3$ $s^{-1}$) is the translocation rate constant of $Val-M^+-CCCP^-$. $K_1$ (∼2 mM for $M^+ = K^+$) is the $CCCP^-$ dissociation constant of $Val-M^+-CCCP^-$ in the membrane, $K_M^*$ (∼25 mM for $M^+ = K^+$ at 100 mM KCl and

pH ~ 7.5) is the apparent metal ion dissociation constant of Val−$M^+$, and $K_{H4}$ (~$10^{-6.5}$ M) is the $H^+$ dissociation constant of CCCPH in the membrane.[27] The concentration of the ternary complex in the inner layer of the vesicular membrane, [Val−$M^+$−CCCP$^-$]$_{il}$, can be determined following the procedure outlined in ref 27. The internal buffer capacity $b_i$ in eq A2 can be calculated using the following expression.[11,27]

$$b_i = (\ln 10)\{\sum C_j K_{Hj}[H^+]/(K_{Hj} + [H^+])^2\} \qquad \text{(A3)}$$

where $C_1$ and $K_{H1}$ are the concentration and proton dissociation constant of the buffer entrapped inside vesicles. $C_2 = 30$ mM, $K_{H2} = 10^{-6.9}$ M and $C_3 = 45$ mM, $K_{H3} = 10^{-7.8}$ M are associated with the endogenous groups in SBPL vesicles. $C_4$ = [CCCP]$_{il}$ and $K_{H4} = 10^{-6.5}$ M.[11] When FCCP is used instead of CCCP, $K_{H4} = 10^{-6.45}$.

The membrane disorder induced by membrane permeant species increases the translocation rate constants by the factor $F$. At the concentrations used in our experiments $F$ is given by the following.[11,27]

$$F = \{1 + B_v[H^+]([Val]_0/[lip])/(10^{-7} + [H^+]) + B_c[H^+]^2([CCCP]_0/[lip])/\{(10^{-7} + [H^+])(K_H + [H^+])\}\} \qquad \text{(A4)}$$

where $B_v \sim 20$ and $B_c \sim 60-90$. The term with [CCCP$^-$]$_{il}$ in the denominator of eq A2 comes because of the condition $\Delta$-[Val]$_{il}$ = $\Delta$[CCCPH]$_{il}$.

In the next step of our strategy, gramicidin is added to the above vesicle solutions, and the change in the $\Delta$pH relaxation rate ($1/\tau_{ch} = 1/\tau - 1/\tau_{VC}$) is noted. Parts of the contributions to $1/\tau_{ch}$ come from mechanisms already studied and known to be contributing in the presence of gramicidin channels: (a) $H^+$/$M^+$ transport through gramicidin channels and $OH^-$ propogation along water chains in the membrane, $1/\tau_G$;[26] (b) $H^+$ translocation as CCCPH and $M^+$ translocation through the gramicidin channels along with CCCP$^-$ translocation through the membrane, $1/\tau_C$;[11] (c) $H^+$ translocation as CCCPH, $M^+$ translocation through the gramicidin channel and CCCP$^-$ translocation as the complex Val−CCCP$^-$ in the membrane, $1/\tau_{VC^-}$.[11]

$$1/\tau_G = (\ln 10/b_i)\{(1.5 \times 10^6/[MCl])([Gram]_0[H^+]/(2[lip]) + 0.04F \times 10^{-7}/(10^{-7} + [H^+])\} \qquad \text{(A5)}$$

$$1/\tau_C = k_c(\ln 10/b_i)F[CCCP^-]_{il} \qquad \text{(A6)}$$

$$1/\tau_{VC^-} = k_4(\ln 10/b_i)F[\text{Val-CCCP}^-]_{il} \qquad \text{(A7)}$$

where $k_c$ in eq A6 is the translocation rate constant of CCCP$^-$ (~2 $s^{-1}$) and [Gram]$_0$ = gramicidin concentration in the vesicle solution. [CCCP$^-$]$_{il}$ and [Val-CCCP$^-$]$_{il}$ are the average concentrations of CCCP$^-$ and Val-CCCP$^-$ in the inner layer of the membrane with translocation rate constants $k_c$ and $k_4$, respectively. Calculations using the parameters estimated in our earlier works show that even at high [CCCP]$_0$ the contributions from eqs A5−A7 are a negligible fraction of $1/\tau_{ch}$.

If $1/\tau_{ch}$ is due to enhancement in the rate of the rate-limiting substep of CCCP$^-$ transport from the "polar region" to "nonpolar region" by schemes I or II, expressions for their contributions $1/\tau_1$ and $1/\tau_2$ can be obtained by a procedure similar to that used earlier.

For the scheme I the linearized rate equation for small deviation from equilibrium $\Delta$[CCCP$_f$]$_{il}$ can be written as follows. (See ref 27 for similar equations and theory.)

$$(-d\Delta[CCCP_f]_{il}/dt) = k_1(\Delta[CCCPH]_{il} - \Delta[CCCPH]_{el}) + k_{21}(\Delta[Val-M^+-CCCP^-]_{il} - \Delta[Val-M^+-CCCP^-]_{el}) \qquad \text{(A8)}$$

Unlike in the mechanism contributing to $1/\tau$ in the absence of gramicidin (eq A2), VAL need not be translocated across the membrane in the mechanism involving scheme I. This enables us to use $\Delta$[Val]$_{il}$ = 0 and write the following for the contribution to $1/\tau_1$ if $H^+$ transport step does not limit the rate of $\Delta$pH decay (as when [CCCPH]$_{il}$ is sufficiently large).

$$1/\tau_1 = \frac{F(\ln 10/b_i)k_{21}[Val-M^+-CCCP^-]_{il}}{\{1 + F([Val-M^+]_{il}/K_1)(k_{21}/k_1)(K_{H4}/[H^+])\}} \qquad \text{(A9)}$$

Because of the condition $\Delta$[Val]$_{il}$ = 0, we do not have a term [CCCP$^-$]$_{il}$[$M^+$]/$K_M$* in the denominator of the expression for $1/\tau_1$ unlike in eq A2. Therefore, unlike $1/\tau_{VC}$, the contribution $1/\tau_1$ does not decrease with increase in [CCCP$^-$]$_{il}$ at higher [CCCP]$_0$. The factor $F$ is included since even in this mechanism translocation of a species, CCCP$^-$, is involved. Since $k_{21} \ll k_1$, the denominator of eq A9 is ~1 when [Val−$M^+$]$_{il}$ is small.

For the scheme II, eq A8 takes the following form.

$$(-d\Delta[CCCP_f]_{il}/dt) = k_1(\Delta[CCCPH]_{il} - \Delta[CCCPH]_{el}) + k_{22}\{\Delta([Val-M^+-CCCP^-]_{il}[CCCP^-]_{il}) - \Delta([Val-M^+-CCCP^-]_{el}[CCCP^-]_{el})\} \qquad \text{(A10)}$$

In this scheme also VAL need not be translocated, and we can use $\Delta$[Val]$_{il}$ = 0. Using eq A1 and expressing [CCCP$^-$]$_{il}$ in terms of [CCCP]$_0$, we can write the following expression for the mechanism involving scheme II.

$$1/\tau_2 = \frac{F(\ln 10/b_i)\{K_{H4}/(K_{H4} + [H^+])\}(2k_{22})[CCCP]_0[Val-M^+-CCCP^-]_{il}}{\{1 + F([Val-M^+-CCCP^-]_{il}/K_1)(2k_{22}/k_1)(K_{H4}/[H^+])\}\{[lip]/0.95\}} \qquad \text{(A11)}$$

Since $k_{22} \ll k_1$, the denominator of eq A11 is ~1 when [Val−$M^+$]$_{il}$ is sufficiently small.

$$1/\tau_{ch} = 1/\tau_1 + 1/\tau_2 \qquad \text{(A12)}$$

## References and Notes


(1) Mitchell, P. *Nature* **1961,** *191,* 144.
(2) Ketterer, B.; Neumcke, B.; Lauger, P. *J. Membr. Biol.* **1971,** *5,* 225.
(3) McLaughlin, S.; Dilger, J. P. *Physiol. Rev.* **1980**, *60*, 825−863 and references therein.
(4) Lauger, P.; Benz, R.; Stark, G.; Bamberg, E.; Jordan, P. C.; Brock W. *Q. Rev. Biophys.* **1981,** *14,* 513−598 and references therein.
(5) Hladky, S. B. *Q. Rev. Biophys.* **1992,** *25,* 459−475 and references therein.
(6) LeBlanc, O. H., Jr. *J. Membr. Biol.* **1971**, *4*, 227.
(7) O'Shaughnessy, K.; Hladky, S. B. *Biochim. Biophys. Acta* **1983,** *724,* 381.
(8) Benz, R.; McLaughlin, S. *Biophys. J.* **1983,** *41,* 381.
(9) Barth, C.; Bihler, H.; Wilheim, M.; Stark, G. *Biophys. Chem.* **1995**, *54*, 127.
(10) Bihler, H.; Stark, G. *Biophys. J.* **1997,** *73,* 746−756 and references therein.
(11) Prabhananda, B. S.; Kombrabail, M. H. *Biochim. Biophys. Acta* **1997,** *1323,* 137.
(12) Paula, S.; Volkov, A. G.; Van Hoek, A. N.; Haines, T. H.; Deamer, D. W. *Biophys. J.* **1996**, *70*, 339.
(13) Parsegian, A. *Nature* **1969,** *221,* 844.
(14) Andersen, O. S.; Fuchs, M. *Biophys. J.* **1975**, *15*, 795.

(15) Neumcke, B.; Lauger, A. *Biophys. J.* **1969**, *9*, 1160.
(16) Haydon, D. A.; Hladky, S. B. *Q. Rev. Biophys.* **1972,** 187.
(17) Cohen, F. S.; Eisenberg, M.; McLaughlin, S. *J. Membr. Biol.* **1977,** *37*, 361.
(18) Krishnamoorthy, G.; Hinkle, P. C. *Biochemistry* **1984,** *23*, 1640.
(19) Tien, H. Ti. *Bilayer Lipid Membranes (BLM);* Marcel Dekker: New York, 1974; p 88.
(20) Simons, R. *Biochim. Biophys. Acta* **1970**, *203*, 209.
(21) Ruf, H. In *Hydrogen Ion Transpsort in Ephitalia;* Schulz, I., Sachs, G., Forte, J. G., Ullrich K. J., Eds.; Elsevier: Amsterdam, 1980; p 11.
(22) Krishnamoorthy, G. *Biochemistry* **1986,** *25*, 6666.
(23) Prabhananda, B. S.; Kombrabail, M. H. *Biochim. Biophys. Acta* **1991**, *1070*, 481.
(24) Seufert, W. D. *Biophysik* **1970,** *7*, 60.
(25) Henderson, P. J. F.; McGivan, J. D.; Chappell, J. B. *Biochem. J.* **1969,** *111*, 521.
(26) Prabhananda, B. S.; Kombrabail, M. H. *Biophys. J.* **1996**, *71*, 3091.
(27) Prabhananda, B. S.; Kombrabail, M. H. *Biochim. Biophys. Acta* **1995,** *1235*, 323.
(28) Seeman, P.; Sha'afi, R. I.; Galey, W. R.; Solomon, A. K. *Biochim. Biophys. Acta* **1970,** *211*, 365.
(29) Amdur, I.; Hammes, G. *Chemical Kinetics;* McGraw-Hill: New York, 1966; p 1.
(30) Funck, Th.; Eggers, F.; Grell, E. *Chimia* **1972,** *26*, 637.
(31) Ahmed, I.; Krishnamoorthy, G. *Biochim. Biophys. Acta* **1990,** *1024*, 298.